Characterization of matrix displacement during embryo implantation

Author: Laura Parra Gutiérrez
Facultat de Física, Universitat de Barcelona, Diagonal 645, 08028 Barcelona, Spain.

Advisors: Amélie Luise Godeau, Elena Martínez Fraiz, Samuel Ojosnegros Martos

Abstract: Embryo implantation is a crucial step in mammalian reproduction. Mechanical forces play an important role in embryo development, but their specific role during implantation has not been established yet. In this work, we analyze the 4D time-lapse data of mouse and human embryos implanting in an *in vitro* set-up to understand the mechanisms embryos use to attach and embed in the matrix. We show that, for both species, mean deformation, strain energy, total force and contractility increase over time. We demonstrate that radial displacement prevails and that more collagen is translocated along the Z axis. Z-displacement is negative underneath the mouse embryos, however human embryos show positive and negative Z-displacement underneath the embryos.

I. INTRODUCTION

In the early stages of mammalian pregnancy, the fertilized ovule undergoes a series of cell divisions and reaches the uterus, where, at the blastocyst stage (early embryonic development structure), it may implant. During implantation, the blastocyst hatches from the zona pellucida, attaches and invades the endometrium. In human reproduction, embryo implantation is a limiting step. While only 25-30% of conceptions lead to successful live births, around 60% of these conceptions are lost during implantation or soon after this process[1]. Mechanical forces and cell contractility play an important role in embryo pre-implantation development[2]. The force generated by the mouse embryos was also shown to facilitate hatching[3]. However, the role of forces during mouse and human embryo implantation has not been established yet due to the inaccessibility of the implantation event.

Despite both being mammalian species, mouse and human embryos have different implantation characteristics. Mouse embryos (ME) attach to the uterine epithelium with the mural trophectoderm (TE) [4] and only invade superficially before the endometrial tissue forms a crypt around the embryo. Whereas, human embryos (HE)attach to the uterine epithelium with the polar trophectoderm located next to the inner cell mass (ICM) (see Fig. 1). Their implantation is interstitial, with the embryo invading into the endometrium[5].

In this work, we study the displacements and forces occurring in a collagen matrix of an *in vitro* set-up where mouse and human embryos implant in order to understand the mechanics of embryo implantation.

II. METHODOLOGY

We have analyzed the 4D (x,y,z,t) time-lapse data of 9 mouse embryo and 14 human embryos implanted in an *in vitro* platform mimicking the physiological conditions of the endometrium.

A. Experimental set up

The experiments were conducted in the laboratory of Dr. Samuel Ojosnegros (Bioengineering in reproductive health, IBEC). Briefly, mouse and human embryos were obtained and cultured following protocols described in [6, 7] with IVC1 IVC2 media. In the following, mouse or human embryos were deposited on top of a thick matrix layer (2D platform) formed by collagen (CellSystems, 5074-35ml) and let to adhere. Time-lapse experiments were done on a Zeiss LSM 780 inverted confocal microscope with x25 or x32 water objectives with 1.4-2 μm Z steps and 20-30 min time interval. Collagen was imaged using light scattering and autofluorescence was induced at 780 nm with 3.5-4 % of a MaiTai laser HP DS.

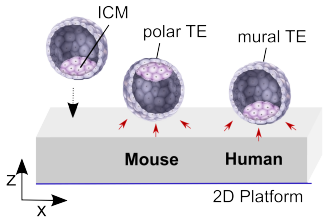

FIG. 1: Schematic representation of embryo implanting in a 2D platform.

B. Software

We used the Python-based open-source software Saenopy to calculate the displacements and forces in the collagen matrix of the different embryos. Saenopy uses 3D image stacks obtained during a period of time and compares each stack to other prior stacks to compute the 3D Cartesian components of the displacements with Particle Image Velocimetry (PIV) and traction forces (derivative of the deformation energy for each tetrahedral finite element into which the mesh is divided) occurring in the collagen matrix. The software simulates a force-free configuration of the collagen matrix, assuming the material is filled with isotropically oriented fibers, exhibiting a certain non-linear stiffness (w'') in function of the strain (λ), constant stiffness (k) and buckling coefficients (d_0 and d_s), according to Eq.(1)[8]. The material parameters were obtained conducting rheological experiments on collagen, increasing the strain from 0-100% at a constant shear rate of 1%/s at 37^{o}C. The stress strain curve was matched to material model parameters and the following values were extracted: k = 1645.0 N/m,

$d_0 = 2.2 \cdot 10^{-3}$, $\lambda_s = 7.5 \cdot 10^{-3}$ and $d_s = 8.1 \cdot 10^{-3}$.

$$w''(\lambda) = \begin{cases} k \exp\left(\frac{\lambda}{d_0}\right) & \text{if } -1 \leq \lambda < 0 \\ k & \text{if } 0 \leq \lambda < \lambda_s \\ k \exp\left(\frac{\lambda - \lambda_s}{d_s}\right) & \text{if } \lambda_s \leq \lambda \end{cases} \quad (1)$$

C. Custom code

With the PIV displacements and forces computed, further analysis was done with the obtained results and custom developed Python code. First, a filter performing the following actions was applied to the deformation to remove artifacts:

1. A maximum filter to filter out values that are abnormally large.
2. A surrounding filter that transforms a certain element to a NaN (Not a Number) if all the surrounding elements are NaNs.
3. A surrounding filter that transforms a certain element to the mean of the surrounding elements if the subtraction between said element and the calculated mean is greater than 0.1μm.

Since the force arrays have a higher number of NaN elements, only the maximum filter has been added to them.

Subsequently, we compute the mean deformation, strain energy (deformation considering the material characteristics), total force (sum of the force vectors, derived from the deformation) and contractility (force components pointing to the force epicenter), as general characteristics of the embryo implantation. To study the specific behavior of each embryo, we follow two main interests: comparing in-plane and out-of-plane displacement and radial to tangential displacement. To study the out-of-plane displacement, we compared the contribution of each Cartesian component to total displacement and computed the variation of the Z-displacement in function of the distance to the embryo. We generated the heatmaps for the average displacement and out-of-plane displacement. On the other hand, to study radial and tangential displacements, we transformed the data into cylindrical coordinates, with the origin of coordinates being the center of deformation of the collagen matrix, and computed the radial and tangential components of the deformation and forces with the aim of comparing both components to discover if one was more significant than the other and their predominant direction (for the radial components, toward or outward the embryo, and, for the tangential components, negative -counterclockwise- or positive -clockwise-).

III. RESULTS

A. Mouse embryo implantation

In Fig. 2 we show a representative example of an implanting mouse embryo (ME1) and the corresponding fiber displacement calculated by PIV. Mouse embryos embed in average (29 ± 10) μm in the collagen matrix until E7.5 (day 8). The top row shows the expansion of ME1 on the collagen surface. The bottom row shows the displacement is directed towards the embryo, indicating a pulling of the collagen matrix by the embryo. As seen in Fig. 3, mean deformation, contractility, strain energy and total force grow over time, as the mouse embryo implants and expands on the surface of the collagen. Since the computed forces for the ME were noisier and had too many NaNs, in this work we have only studied the latter for ME. The order of the deformation vectors ranges from 10^{-2} to 10 μm.

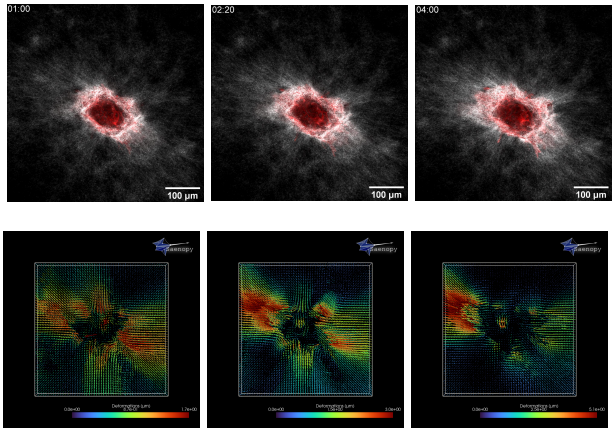

FIG. 2: Evolution of ME1 through time, shown at t=1:00 h, t=2:20 h and t=4:00 h. *Top:* Microscope image. Embryos express membrane-bound tdTomato (red). The collagen matrix fibers were acquired using light scattering. *Bottom:* Deformation vectors computed with Saenopy (top view).

1. *In-plane versus out-of-plane displacement*

To study the variation of displacement with relation to its distance from the embryo, we plotted heatmaps of mean deformation in each coordinate (Fig. 5a, ME2 as example). In all ME, we observed the largest deformation in the collagen around and underneath the embryos. Knowing displacement is directed towards the embryo, we wanted to study if the embryo pulls equivalently in each direction. In order to do that, we split the displacement in in-plane (X, Y) and out-of-plane (Z) components. In Fig. 5b, we plot the ratio of Z to total displacement for the different ME. Although we observe a great variability of the computed ratio, most of the embryos exhibit a higher out-of-plane component (ratio>0.3). In the majority of embryos, the out-of-plane displacement is more significant at the start of the experiment and equalizes with the other components over time. This can be explained by ME first penetrating in the matrix and then spreading on the surface when implanting. This suggests that embryo spreading on the surface is associated to in-plane displacements. Generally, embryos implanted in presence of Dasatinhib exhibit a greater ratio, due to the lack of expansion on the collagen surface. Figure 5c shows

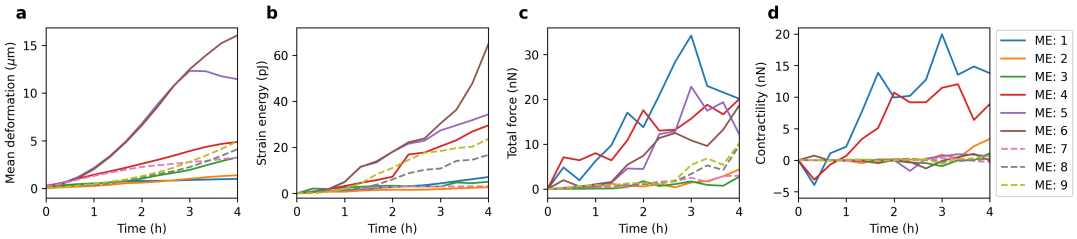

FIG. 3: (a) Mean deformation, (b) strain energy, (c) total force and (d) contractility vs. time. The dashed lines correspond to embryos implanted in the presence of Dasatinhib (drug that inhibits adhesion molecules, thus limiting expansion of the embryo).

the Z displacement in relation to the position of the embryo. We observe negative displacement of the collagen in the laterals and underneath the embryo and positive Z displacement further from it. We concluded ME push the collagen beneath and adjacent to them, and pull towards them the upper and distant layers of the matrix.

2. *Radial versus tangential displacement*

As ME spread on the collagen surface, we wondered what mechanisms the embryos used to achieve this expansion. For this reason, we studied the in-plane displacement of the matrix. First, we calculated the displacement relative to the center of forces of the ME, then we split in-plane deformation into radial and tangential components. In Fig. 8a, we observe the evolution of mean radial and tangential deformation over time (for ME1, as a representative example). While mean radial deformation increases with time, mean tangential deformation remains close to 0. We observed that, on average, the radial component was always more significant than the tangential component of each vector, and pointed towards the embryo. Yet, we were interested in the tangential component of the deformation, as it could be an evidence for ME rotation, which in turn might contribute to the Z-displacement of the mouse embryo into the matrix. In Fig. 8c, we plot the ratio of the sum of clockwise to counterclockwise direction of the tangential component of in-plane displacement. We observe variability in the preferred direction, as clockwise, counterclockwise, and the ratio=1 (no net tangential movement) represent each 33%. However, since the tangential displacement is negligible compared to the radial component, a rotation of the ME could not be detected. Nevertheless, the tangential component could help to explain tangential remodeling of collagen underneath the embryo.

B. Human embryo implantation

In Fig. 4, we show a representative example of an implanting human embryo (HE) and the corresponding fiber displacement and force vectors. The growth and the embedding of the HE in the collagen is visible, as the bottom of the embryo descends deeper (Fig. 4 first row) and the surface of the HE becomes larger (Fig. 4 second row). Similarly to the mouse embryo, the displacement is directed towards the embryo, indicating a pulling of the collagen matrix. As shown in Fig. 6, as for mouse embryos, mean deformation, strain energy, total force and contractility grow over time as the human embryos implant in the collagen substrate, reaching up to 30 μm and 12.5 μN. More implanted embryos (D9/D10) show a lower deformation than embryos at an earlier implantation stage (D8). Overall, HE show higher displacements than ME.

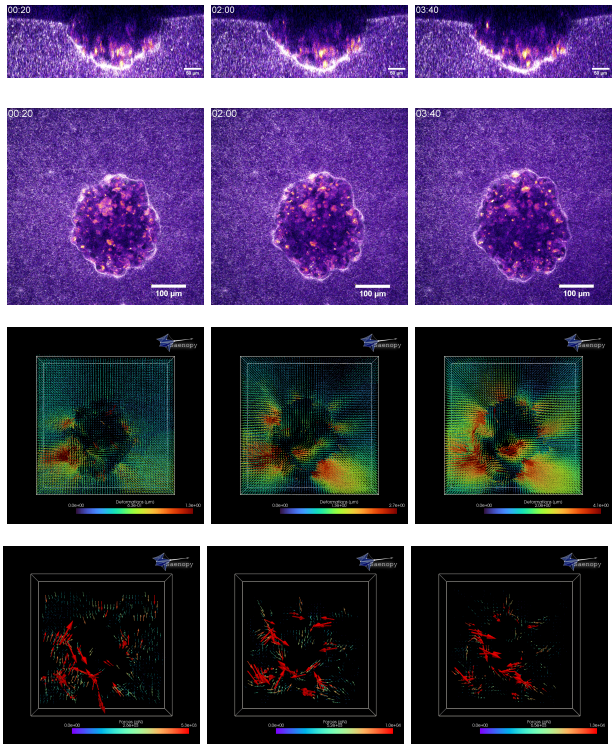

FIG. 4: Evolution of HE23 through time, shown: t=0:20 h, t=2:00 h and t=3:40 h. *From top to bottom:* Time-lapse images of (1) lateral view and (2) top view of implanting human embryo. The collagen matrix, fibers, and deformations were acquired using light scattering. The embryo image was captured using autofluorescence and multiphoton illumination. (3) Deformation vectors were calculated with PIV (top view). (4) Force vectors were computed with Saenopy (top view).

1. *In-plane versus out-of-plane displacement*

Figure 7a (HE50.1 as example), shows the displacement is greater underneath and around the human embryos. In order to understand how HE partially embed in

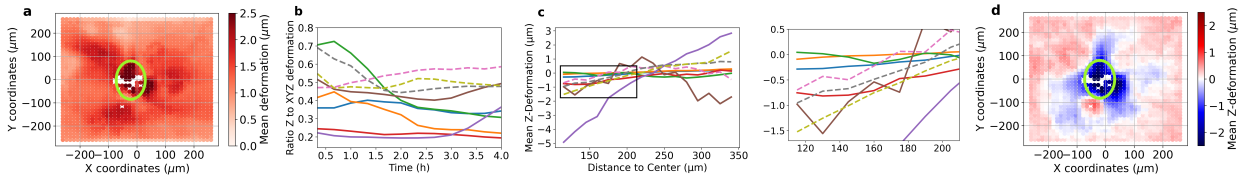

FIG. 5: (a) Representative heatmap of mean total deformation (ME2). (b) Absolute out-of-plane deformation to total deformation ratio vs. time. Only the first 4 hours of data have been selected due to increasing loss of data in the following time points. (c) Mean value of out-of-plane deformation vs. in-plane radius, with close-up of the squared region on the right (legend in Fig. 3.) (d) Representative heatmap of mean in-plane deformation (ME2). Green outline: approximate position of the embryo. Dashed lines: embryos implanted in the presence of Dasatinhib.

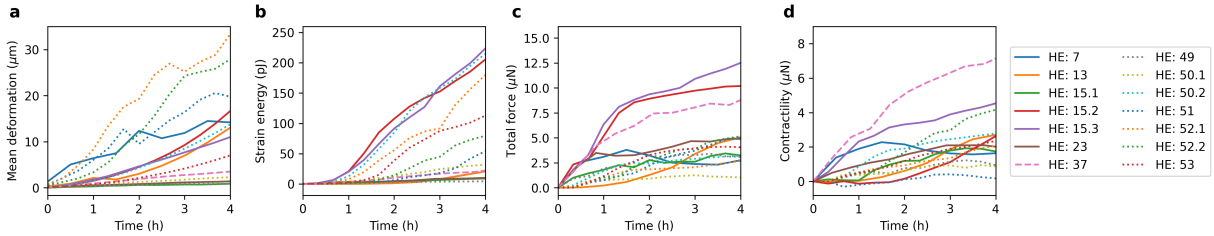

FIG. 6: Mean deformation (a), strain energy (b), total force (c) and contractility (d) vs. time. The dashed lines correspond to older embryos (imaged on day 10 after fertilization), the dotted lines correspond to younger embryos (imaged on day 8), the rest of the embryos were imaged on day 9.

the collagen matrix, we split the deformation in in-plane and out-of-plane components. In Fig. 7b, we observe the ratio of Z displacement compared to total displacement for all embryos, except HE7 and HE37, is greater than 0.3, meaning z component is the most significant for HE. The embryos with lowest Z ratio were imaged on day 9 and 10, suggesting a decrease in out-of-plane component or an increase of in-plane component with progression of implantation over time. In Fig. 7c, we see how the mean out-of-plane displacement changes in function of the distance to the embryo. In the studied human embryos, we observe two different behaviors. In HE 15.1, 15.2 and 23, (Fig. 7e) we find positive displacement underneath and in the lower layers of the collagen closer to the embryo suggesting the embryo is pulling the collagen as it embeds. However, in the remaining HE, displacement underneath and around the embryo is completely negative (Fig. 7d) suggesting that the embryo pushes the collagen. Further away from the embryo, there is a greater variability in the direction of the out-of-plane deformation. We can relate the direction of the Z displacement around the embryo to the implantation stage. Younger embryos (D8) have the greatest negatives values of deformation, while all the embryos that pull the collagen underneath them (positive Z displacement), are older (D9). Nonetheless, both types of embryos presented descent into the collagen. We hypothesize that, in the first days of implantation, HE push the collagen below them to penetrate as much as they can and, in later stages of the process, start pulling the collagen in the bottom as well.

2. *Radial versus tangential displacement*

As human embryos integrate into the matrix, we asked if this was associated to a symmetry breaking such as a rotation. Therefore, we looked at the radial and tangential component relative to the embryo center of the force the embryo exerts on the matrix. In Fig. 8b, similarly to ME, we observe the radial component of the in-plane force increases with time, while the tangential component fluctuates around 0. In HE, we too observed that, on average, likewise to ME, the radial component is always more significant than the tangential component of each vector, and pointed towards the embryo. To see if we detected rotational movement, we plotted Fig. 8d. We observe a similar variability in the preferred direction of the embryo to the one observed in ME, however, with a less constant ratio for each embryo. In Fig. 8e, we observe peaks in clockwise counterclockwise tangential movement, this suggests that a local contraction of the embryo pulls the collagen to the contraction center. Considering the small contribution of the tangential component and the fluctuation of the clockwise/counterclockwise ratio, consistent rotation of the embryo could not be confirmed.

IV. CONCLUSIONS

In this work, we study the displacements of the collagen matrix and the role of forces exerted by mouse and human embryos during implantation in order to better understand the mechanics of embryo implantation. In contrast to mouse embryos that attach and spread on the surface, human embryos invade the matrix and embed partially. In agreement, we have observed differences in the out-of-plane displacement of the two species. We saw that the deformation generated by human embryos is generally larger than the one's generated by mouse embryos. Nonetheless, we have found similarities in the implantation of both kinds. First, for mouse and human embryos, the radial component was more significant than

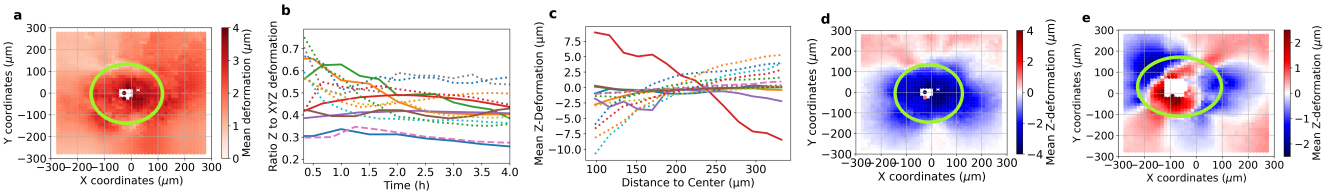

FIG. 7: (a) Representative heatmap of mean total deformation (HE50.1). (b) Absolute out-of-plane deformation to total deformation ratio vs. time. Only the first 4 hours of data have been selected due to increasing loss of data in the following time points. (c) Mean value of out-of-plane deformation vs. in-plane radius (legend in Fig. 6). (d) Representative heatmap of Z-displacement deformation (HE50.1, day 8 imaging). (e) Representative heatmap of mean Z-displacement (HE23, day 9 imaging). Green outline: approximate position of the embryo. Dashed lines: older embryos (imaged on day 10 after fertilization, dotted lines: younger embryos (imaged on day 8), otherwise imaged on day 9. Embryos were deposited on the matrix on day 5 or 6 post-fertilization.

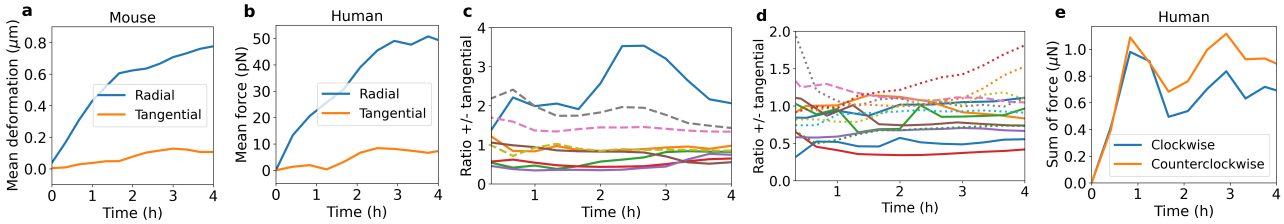

FIG. 8: (a) Representative example of average in-plane deformation in radial and tangential components for each vector vs. time for mouse embryos (ME1). (b) Representative example of average in-plane force in radial and tangential components for each vector vs. time for human embryos (HE1). (c) Clockwise to counterclockwise directions' sum ratio for in-plane deformation vectors vs. time for ME (legend in Fig. 3). (d) Clockwise to counterclockwise directions' sum ratio for in-plane deformation vectors vs. time for HE (legend in Fig. 6). (e) Representative example of sum of clockwise and sum of counterclockwise tangential forces vs. time for human embryos (HE23).

the tangential component. Second, in both species the maximal displacement was located nearby the embryos and the out-of-plane component was the most significant. However, while all the studied mouse embryos presented negative Z displacement underneath and around them, human embryos presented two different behaviors potentially related to their implantation stage. At earlier time points, embryos seem to push the collagen underneath them (negative displacement) and, at later time points of implantation, embryos seem to pull the collagen (positive displacement).

Overall, we have seen that the forces play a significant role in embryo implantation. However, how similar displacement patterns can lead to two different implantation behaviors, (i) spreading on the surface and (ii) embedding in the matrix, remains an open question to be addressed in the future.

Acknowledgments

I would like to express my sincere gratitude to my advisors, Dr. Amélie Godeau and Dr. Elena Martínez, for their guidance in this fascinating work. To Dr. Samuel Ojosnegros and his group for welcoming me in their lab, and David Böhringer, for his help with the Saenopy software. Lastly, to my friends and family for their support.

[1] T. Chard, "Frequency of implantation and early pregnancy loss in natural cycles," *Baillière's Clinical Obstetrics and Gynaecology*, vol. 5, no. 1, pp. 179–189, 1991.

[2] O. Özgüç *et al.*, "Multiscale morphogenesis of the mouse blastocyst by actomyosin contractility," *Current Opinion in Cell Biology*, vol. 66, pp. 123–129, 2020. Cell Dynamics.

[3] K. Leonavicius *et al.*, "Mechanics of mouse blastocyst hatching revealed by a hydrogel-based microdeformation assay," *Proceedings of the National Academy of Sciences*, vol. 115, no. 41, pp. 10375–10380, 2018.

[4] K. Y. Lee *et al.*, "Animal models of implantation," *Reproduction*, vol. 128, no. 6, pp. 679 – 695, 2004.

[5] J. Muter *et al.*, "Human embryo implantation," *Development*, vol. 150, p. dev201507, 05 2023.

[6] I. Bedzhov *et al.*, "In vitro culture of mouse blastocysts beyond the implantation stages," *Nature protocols*, vol. 9, pp. 2732–9, 12 2014.

[7] M. Shahbazi *et al.*, "Self-organization of the human embryo in the absence of maternal tissues," *Nature cell biology*, vol. 18, 05 2016.

[8] D. Böhringer *et al.*, "Dynamic traction force measurements of migrating immune cells in 3d matrices," *bioRxiv*, 2023.